

# Study on the Properties of the Electrospun Silk Fibroin/Gelatin Blend Nanofibers for Scaffolds

Yin-Guibo,<sup>1,2</sup> Zhang-Youzhu,<sup>1</sup> Bao-Weiwei,<sup>1</sup> Wu-Jialin,<sup>1</sup> Shi De-bing,<sup>3</sup>  
Dong Zhi-hui,<sup>3</sup> Fu Wei-guo<sup>3</sup>

<sup>1</sup>School of Material Engineering, Soochow University, Suzhou 215021, People's Republic of China

<sup>2</sup>Department of Textile, Nantong Textile Vocational Technology College, Nantong 226007, People's Republic of China

<sup>3</sup>Department of Vascular Surgery, Zhongshan Hospital, Fudan University, Shanghai 200032, People's Republic of China

Received 10 October 2007; accepted 29 June 2008

DOI 10.1002/app.28963

Published online 30 October 2008 in Wiley InterScience (www.interscience.wiley.com).

**ABSTRACT:** Silk fibroin (SF)/gelatin blend nanofibers membranes as scaffolds were fabricated successfully via electrospinning with different composition ratios in formic acid. The formation of intermolecular hydrogen bonds and the conformational transition of SF provided scaffolds with excellent mechanical properties. FTIR and DTA analysis showed the SF/gelatin nanofibers had more  $\beta$ -sheet structures than the pure SF nanofibers. The former's breaking tenacity increased from 0.95 up to 1.60 MPa, strain at break was 7.6%, average fiber diameter was 89.2 nm, porosity was 87%, and pore diameter was 142 nm. MTT, H&E stain, and SEM results showed that the adhesion, spreading, and proliferation of human umbilic vein endothelium cells (HUVECs) and mouse fibroblasts on the

SF/gelatin nanofibers scaffolds were definitely better than that on the SF nanofibers scaffolds. The scaffolds could replace the natural ECM proteins, support long-term cell growth, form three-dimensional networks of the nanofibrous structure, and grow in the direction of fiber orientation. Our results prove that the addition of gelatin improved the mechanical and biological properties of the pure SF nanofibers, these SF/gelatin blend nanofiber membranes are desirable for the scaffolds and may be a good candidate for blood vessel engineering scaffolds. © 2008 Wiley Periodicals, Inc. *J Appl Polym Sci* 111: 1471–1477, 2009

**Key words:** electrospinning; nanofibers; silk fibroin; gelatin; scaffolds

## INTRODUCTION

Without autologous transfer of tissue or a valid alternative for tissue replacement, it is difficult to regenerate and reconstruct bone, nerve, blood vessel, skin, heart, or skeletal muscle because of continuous accidental injuries. However, tissue engineers develop a new approach to solve this problem. The principle of the tissue engineering is first to mimic the fibrillar structure of the extracellular matrix (ECM) that provides essential guidance for cell organization, survival, and function and then to develop feasible substitutes to aid in the clinical treatment.

Biomaterials composition and morphology play a pivotal role in tissue engineering by serving as membranes for cellular ingrowth, proliferation, and new tissue formation. Three-dimensional nanofibrous scaffolds are regarded as ideal material for tissue engineering because they can not only mimic the nanosized dimension of natural ECM but can also form a defined

architecture to guide cell growth and development as needed. At present, three different techniques are used to prepare such scaffolds: self-assembly, electrospinning, and phase separation. By changing process parameters, electrospinning can freely control scaffold structure properties such as fiber diameter and porosity, therefore it is especially good at enabling us to mimic the ECM. Polymeric liquids in solution or molten form are elongated and split continuously by high-voltage electrostatic fields. With different collecting methods, electrospinning can prepare random or oriented nanofiber membranes (or vessels).

Silk fibroin (SF) has excellent biocompatibility with other nontoxic and noninflammatory products that biodegrade and become replaced *in vivo*. Kim<sup>1</sup> fabricated SF nanofiber membrane, and Min<sup>2</sup> further investigated the cell activities of normal human keratinocytes and fibroblasts on SF nanofiber scaffolds. Collagen is the key structural protein in ECM. Gelatin is a natural biopolymer derived from collagens and can be easily extracted from animal tissue such as skin, cartilage, and bone. Gelatin and collagens have almost the same compositions and biological properties.<sup>3</sup>

Some researchers found that pure gelatin or SF nanofiber membrane is water soluble and mechanically weak.<sup>4</sup> It can neither be singly used to replace the natural ECM proteins before host cells

Correspondence to: Zhang-Youzhu (zhangyouzhu@suda.edu.cn).

Contract grant sponsor: Chinese Jiangsu Province Key Lab Foundation; contract grant number: S8115033.

repopulate nor resynthesize a new, but different natural matrix. In addition, when the SF nanofiber component is alone, it is difficult to regulate proliferation and differentiation of cells. However, few investigations have been attempted to electrospin blend SF/gelatin nanofibers, further studies on the biological application have not been found.

This study aims to modify the mechanical and biological properties of SF nanofibers with gelatin and further investigate the feasibility for engineering blood vessel scaffolds. We first add the gelatin to the SF solution to improve viscosity and spinnability and obtain nanoscale blend fibers by optimizing the processing parameters. Second, we characterize nanofibers microstructure by FTIR and DTA and test their mechanical property, porosity, pore diameter. Finally, we investigate the responses in cultures of human umbilic vein endothelium cells (HUVECs) and mouse fibroblasts on different membranes.

## EXPERIMENTS

### Electrospinning

The air-dried regenerated SF membrane blended with gelatin in different ratios (100 : 0, 90 : 10, 80 : 20, 70 : 30, 60 : 40, 50 : 50, w/w). Both of them were dissolved in 98 wt % formic acid to obtain 10–16 wt % concentrations. For electrospinning, a high electric potential was applied to a droplet of solution at the tip (ID 0.8 mm) of a syringe needle in a horizontal mount. The electrospun nanofibers were collected on stainless mesh connected with a cathode. The distance between the needle tip and the collector ranged from 7 to 18 cm and could be adjusted. The electrospun nanofiber membranes were inserted into 100% methanol for 10 min to form chemically treated nanofiber membranes as controls.

### Characterization of morphology

The morphologies of the electrospun fibers were observed by a Hitachi S-570 SEM (scanning electron microscope), with magnification of 10,000. The average fiber diameters and standard deviation (STDEV) were calculated by analyzing the SEM images with a custom code image analysis program (Adobe Photoshop 7.0).

### Characterization of microstructure

FTIR spectra were obtained by using a series spectrometer (Nicolet 5700, PE LO. USA) in the spectral region of 4000–400  $\text{cm}^{-1}$ ; DTA curves were obtained through a thermal analysis instrument (Diamond 5700, PE Co. USA) at a heating rate of 10°C/min, scan range of 40–400°C, and nitrogen gas flow rate of 120 mL/min.

### Mechanical property

The tensile testing was performed by using an Instron tester (Model 3365). The length of samples was 30 mm and the width was 6 mm. The cross-head speed was 20 mm/min, five samples in each group. The mechanical property was characterized according to the following formula:

$$\text{Breaking tenacity} = \frac{\text{breaking strength (N)}}{\text{thickness (mm)} \times \text{width (mm)}} \quad (1)$$

$$\text{Strain at break(\%)} = \left( \frac{L_1 - L_0}{L_0} \right) \times 100 \quad (2)$$

where  $L_0$  was the length of sample,  $L_1$  was the length at break.

### Porosity and pore diameter

We calculated the porosity according to the method described by Vaz et al.<sup>5</sup> According to the SEM photograph, the area of the pore was calculated and then converted into one of circle. The circular diameter was regarded as the pore diameter,<sup>5,6</sup> three samples in each group. The porosity ( $\epsilon$ ) was calculated from the measured average density of the samples and the standard density of SF/gelatin ( $\rho_0 = 1.1 \text{ g/cm}^3$ ).

$$\epsilon(\%) = \left( 1 - \frac{\rho}{\rho_0} \right) \times 100 \quad (3)$$

where  $\rho$  is average density and  $\rho_0$  is standard density (70 : 30)

### Cell culture

The air-dried SF membrane, SF and SF/gelatin nanofiber membranes were cut out and sterilized by  $\gamma$  ray and put onto 24-well plates. HUVECs and mouse fibroblasts were cultured at a density of  $5 \times 10^4$  well in RPMI 1640 medium containing 10% fetal bovine serum, 2 mM L-glutamine, 100 U/mL penicillin, and 100  $\mu\text{g/mL}$  streptomycin. The cell culture was maintained at 37°C in a humidified 5%  $\text{CO}_2$  incubator, according to the methods described by Jin et al.<sup>7</sup>

### Analysis

Mouse fibroblasts cultures were photographed using OLYMPUS CKX31 after 12, 24, 48, and 72 h of cell culture. HUVECs cultures were monitored after 6, 12, 24, 36, and 48 h by the mitochondrial metabolic MTT assay, and the absorbance at 450 nm was measured by a spectrophotometer. HUVECs were

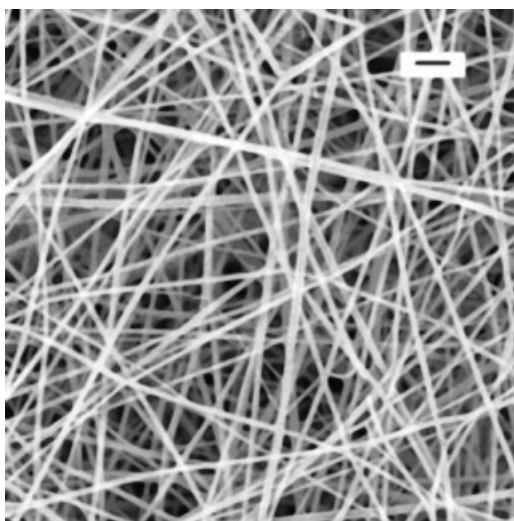


**Figure 1** SEM of SF/gelatin blend nanofibers manufactured with the optimum process, concentration 11%, ratio 70 : 30, distance 13 cm, voltage 22 kV, scale bar: 600 nm

stained with Hematoxylin and Eosin (H&E) and photographed using light microscopy after 24, 48 h of cell culture. HUVECs were observed under SEM after 5, 21 days of cell culture.

## RESULTS AND DISCUSSION

### Morphology of SF/gelatin nanofibers

The viscosity of SF/gelatin blend solution is higher than pure SF solution, consequently the spinnability of blend solution improves, which makes it easy for the splitting and draft of jet flow. When the blend proportion was kept at 70 : 30 (w/w), the solution had the best spinnability. Figure 1 showed the nanofibers were homogeneous, nonbeaded, and continuous. Average fiber diameter reached 83.9 nm by optimizing the electrospinning process parameters such as electrode distance, voltage, concentration of solution, etc.

### Microstructure

FTIR spectroscopy is used to follow the conformational changes that occur during the electrospinning process. Random coils show strong absorption bands at 1650–16605  $\text{cm}^{-1}$  of amide I ( $\nu_{\text{C=O}}$ ), 1535–1545  $\text{cm}^{-1}$  of amide II ( $\delta_{\text{N-H}}$ ) and the  $\beta$ -sheets show absorption bands at 1625–1640  $\text{cm}^{-1}$  of amide I, 1515–1525  $\text{cm}^{-1}$  of amide II.<sup>8</sup> Figure 2(1) showed IR spectra of nanofiber membranes. SF nanofibers showed two absorption bands at 1654.5 (amide I) and 1541.6  $\text{cm}^{-1}$  (amide II), which can be attributed to the random coil conformation. In contrast with SF nanofibers, although the characteristic absorption bands of SF/gelatin nanofibers were observed at

1654.8 and 1541.8  $\text{cm}^{-1}$ , indicative of the random coil conformation, the electrospun SF/gelatin blend nanofibers mainly showed a transition to the characteristic absorption bands at 1630.6 and 1523.4  $\text{cm}^{-1}$  ( $\beta$ -sheet), in particular, the intensity of absorption peaks was obviously elevated, which indicated some random coils converted into stable  $\beta$ -sheets. In Figure 2(3), we observed chemically treated SF/gelatin nanofibers showed strong absorption bands at 1630.1 and 1523.9  $\text{cm}^{-1}$ , indicating the  $\beta$ -sheet conformation. After treatment with chemicals, Kim and Park also found that the characteristic absorption bands of chemically treated SF nanofibers shifted from 1653 (amide I) to 1541  $\text{cm}^{-1}$  (amide II) to low wave numbers, and the SF molecules mainly showed the  $\beta$ -sheet conformations.<sup>2,9</sup> It was well known that SF macromolecules can rearrange to form crystalline structures due to changes in hydrogen bonding caused by chemicals such as methanol, glutaraldehyde, and ethanol. From this viewpoint, we can also assume that the conformational transition of SF in the electrospun SF/gelatin nanofibers can also be created due to hydrogen bonding formed between N–H, O–H, and C=O groups in peptide chains. Gelatin, a denatured substance from collagen involving rupture of the triple-helix structure by breaking of hydrogen bonds and a rearrangement of the triple-helix into a random configuration, can undergo a conformational disorder-order transition to recover the triple-helix structure under proper conditions.<sup>4</sup> From the spectra of the electrospun SF/gelatin blend nanofibers as shown in Figure 2(2), we are difficult to discern the gelatin conformation. However, Ki found that the electrospun gelatin nanofiber exhibited a mixture of  $\alpha$ -helical and random coil

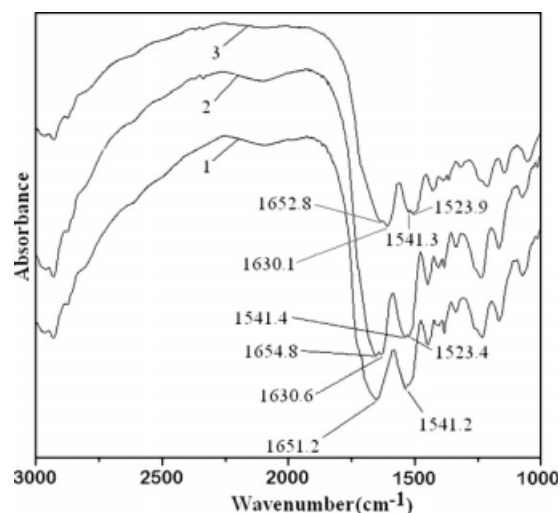


**Figure 2** The IR spectra of SF nanofibers (1), SF/gelatin blend nanofibers (2), chemically treated SF/gelatin nanofibers (3).

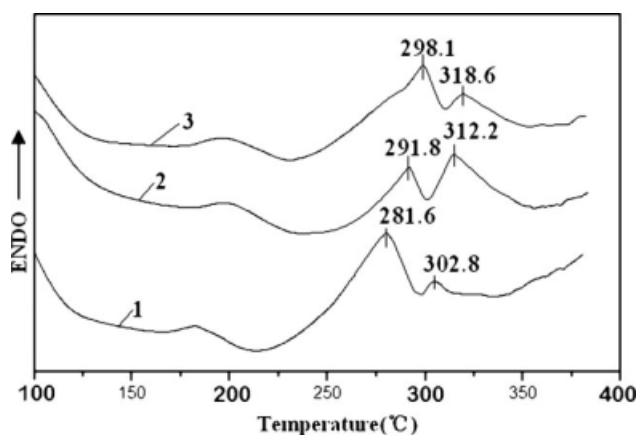


**Figure 3** DTA curves of SF nanofibers (1), SF/gelatin blend nanofibers (2), chemically treated SF/gelatin nanofibers (3).

conformation.<sup>10</sup> Furthermore, Zhang et al. found that the crosslinking treatment with glutaraldehyde vapor enhanced the content of helix structure of the electrospun gelatin fibers, which is primarily dependent on the special features of the peptide bonds involving the imino acids, supplemented by inter-chain hydrogen bonds at the positions occupied by glycine.<sup>4</sup> It should be noted that the content of glycine normally reaches 36–45% in the SF macromolecules, therefore we speculate the gelatin molecules in SF/gelatin blend nanofibers still show a mixture of  $\alpha$ -helical and random coil conformation; however, the content of helix structures may be increased due to the hydrogen bonds within molecules.

Magoshi and Magoshi found that the thermal decomposition temperature of SF (random coils) was 290–300°C.<sup>11</sup> Figure 3 showed that SF nanofibers had two thermal absorption peaks at about 281.6 and 310.23°C, the intensity of the latter was lower, indicating the random coil conformations. The electrospun SF/gelatin nanofibers showed peaks at 291.80 and 313.22°C, particularly the intensity of the peak at 313.22°C drastically increased. Additionally, the thermal stability of the electrospun SF/gelatin fibers was close to that of chemically treated SF/gelatin nanofib-

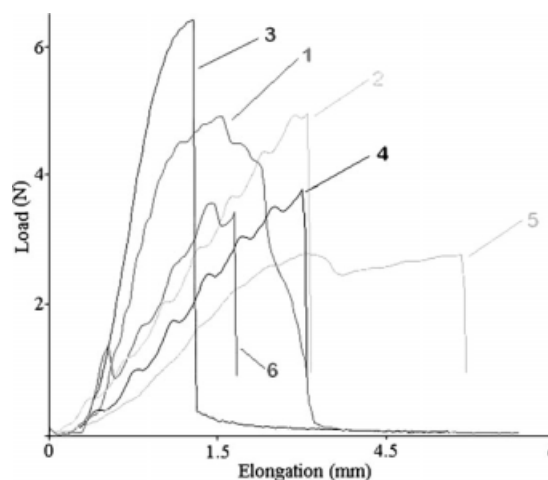


**Figure 4** Load-elongation curves of the electrospun nanofiber membranes: (1), (2), (3) SF/gelatin nanofiber membranes (70 : 30), the concentrations 10, 13, and 16 wt %, respectively; (4) SF/gelatin nanofiber membranes (50 : 50), the concentrations 13 wt %; (5) SF nanofiber membranes, the concentration 13%; (6) No. 2 sample was chemically treated with methanol for 10 min.

ers whose peaks were at 298.05 and 318.60°C ( $\beta$ -sheet thermal decomposition absorption peaks), we can also prove the addition of gelatin resulted in relatively easy crystallization and increased  $\beta$ -sheet content, this result was consistent with FTIR analysis.

### Mechanical property

To investigate the feasibility for scaffolds, mechanical properties of SF/gelatin nanofibers membranes were characterized. Load-elongation curves were plotted in Figure 4. Based on the load-elongation curves, breaking tenacity and strain at break were summarized in Table I. The breaking tenacity increased from 0.95 MPa, 1.60 to 2.70 MPa with increasing the content of gelatin from 0%, 30 to 50%. By the addition of gelatin, intermolecular hydrogen bonds formed between SF and gelatin molecules increased, therefore many random coil conformations of SF converted into  $\beta$ -sheet ones, which was responsible for the increase of breaking tenacity. After the

**TABLE I**  
Mechanical Property of SF/Gelatin Nanofibers Membranes

No.	SF/gelatin (w/w)	Concentration (%)	Thickness (mm)	Breaking tenacity (MPa)	Strain at break (%)
1	70 : 30	10	0.31	1.48 ± 0.21	5.9 ± 1.22
2	70 : 30	13	0.28	1.60 ± 0.14	7.6 ± 1.91
3	70 : 30	16	0.23	2.25 ± 0.11	5.7 ± 1.03
4	50 : 50	13	0.12	2.70 ± 0.34	4.2 ± 1.84
5	100 : 0	13	0.28	0.95 ± 0.28	7.5 ± 2.09
6	Control <sup>a</sup>	13	0.06	4.13 ± 0.65	3.5 ± 1.41

<sup>a</sup> No. 2 sample was treated with 100% methanol for 10 min as a control.

**TABLE II**  
**Porosity and Pore Diameter of SF/Gelatin Nanofibers Membranes with Different Concentrations (70 : 30)**

Concentration (%)	Thickness (mm)	Average diameter (nm)	Density (g/m <sup>3</sup> )	Porosity (%)	Pore diameter (nm)
10	0.30	112 ± 13	0.12	89 ± 4.45	86 ± 5.20
13	0.29	163 ± 19	0.14	87 ± 6.29	142 ± 6.91
16	0.30	275 ± 27	0.16	85 ± 3.81	250 ± 8.26

treatment with methanol, the IR results indicated that the random coils converted into the  $\beta$ -sheet conformation, so the breaking tenacity was further elevated; however, the treatment with methanol reduced the extension ability, the strain at break of chemically treated membranes decreased nearly 50% lower than those of the electrospun SF/gelatin membranes, which showed chemically treated membranes became crisp. In contrast, the electrospun SF/gelatin membranes remained excellent elasticity, the strain at break was up to 7.6%, which proved the addition of gelatin both improved tensile strength of pure SF nanofibers membrane and obtained excellent elasticity. In addition, the breaking tenacity increased from 1.48 MPa, 1.60 to 2.25 MPa with increasing concentrations of solution from 10%, 13 to 16%. As summarized in Table II, we found that the nanofiber diameters increased with increasing the concentration of spinning solutions, which may be responsible for this improvement.

#### Porosity and pore diameter

As shown in Table II, at the low concentration, nanofiber diameters were smaller and they aggregated closely, so pore diameters grew smaller. Porosity ranges from 85 to 89% are desirable for the scaffolds and facilitates the spreading and proliferation of cells.

#### Property of cell culture

Observation of mouse fibroblasts using light microscopy

Figure 5 showed that SF air-dried membranes, SF and SF/gelatin nanofiber membranes could support

adhesion and growth of mouse fibroblasts after 12 h of cultivation. SF is an electronegative protein, its crystalline and amorphous regions coexist. Some researches suggested that electronegative biomaterials had good biocompatibility. In addition, SF amorphous regions consist of many alkaline amino acids, which also tend to adsorb cells.<sup>12</sup>

Figure 5 showed that the number of the cells on SF and SF/gelatin nanofiber membranes were significantly higher than that on the SF air-dried membrane. The phenomenon suggested the electrospun nanofiber membranes, which have higher volume-to-surface and porosity, could provide a three-dimensional structure for cell growth and proliferation compared to SF air-dried membranes whose surfaces are smooth. Figure 5 showed that mouse fibroblasts gathered and demonstrated spherical shape on the SF air-dried membranes. However, the cells seeded on SF/gelatin nanofibers scaffolds were shuttle shape, which demonstrated that the spreading of mouse fibroblasts on SF/gelatin nanofibers scaffolds were definitely better than that on the SF nanofiber scaffolds because of the addition of gelatin.

#### Observation of H&E stain

HUVECs could grow on the SF air-dried membranes, SF and SF/gelatin nanofiber membranes. After 24 h of cultivation, most cells on the SF air-dried membranes and SF nanofiber membranes were spherical shaped and few were shuttle shape. HUVECs proliferated significantly, and the number of shuttle-shape cells increased after 48 h of cultivation on SF, SF/gelatin nanofiber membranes.

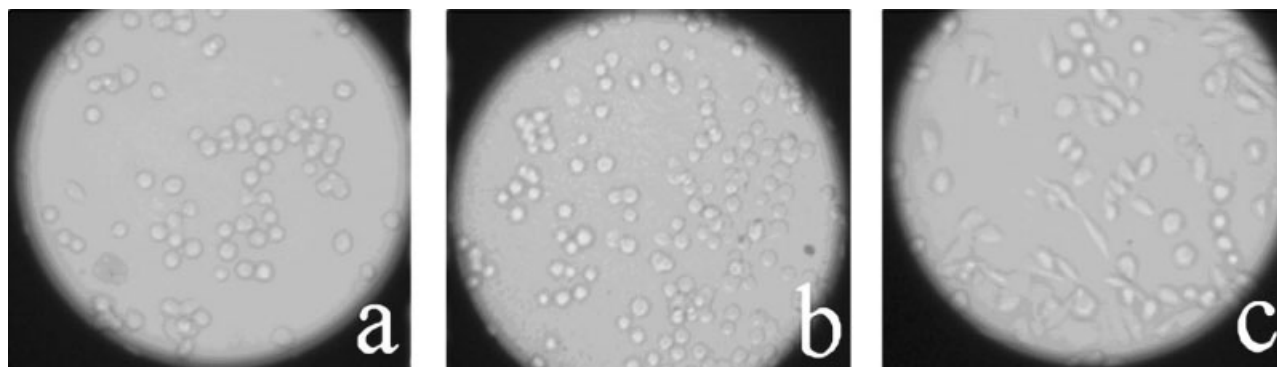


**Figure 5** Microscopy images of mouse fibroblasts after 12 h of cultivation.

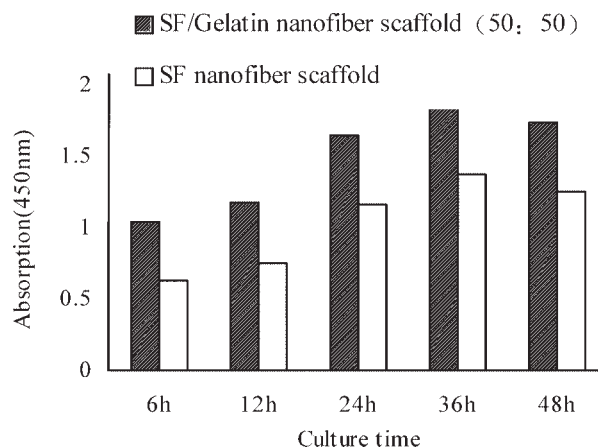


**Figure 6** Proliferation curves of HUVECs on different nanofiber membranes.

Moreover, whether the time of cultivation was 24 or 48 h, the number of the HUVECs (especially the cells of shuttle shape) on SF and SF/gelatin nanofibers membranes were significantly higher than on the SF air-dried membranes. This phenomenon similarly suggested that electrospun nanofiber scaffolds favored cell proliferation and growth because of their high surface-to-volume, porosity, and three-dimensional structure. Most cells on the SF/gelatin nanofiber membranes demonstrated shuttle shape, the spreading of these cells on SF/gelatin nanofiber membranes excelled that on the SF nanofiber membranes.

#### MTT assay

To further quantify the cell proliferation, MTT assay was performed, the absorbance intensity at 450 nm of SF, SF/gelatin nanofiber membranes was shown in Figure 6. Absorbance is in proportion to the number of the active cells, as shown in Figure 6, the numbers of HUVECs on SF and SF/gelatin nanofiber membranes were significantly increased after 36 h of

cultivation, which suggested that HUVECs could grow and proliferate on the nanofiber scaffolds. The number of the HUVECs on SF/gelatin nanofiber membranes was significantly higher than that of the SF nanofiber membranes, which also proved that, as a bioactive protein and a product degraded from collagen, the gelatin could promote cell proliferation.

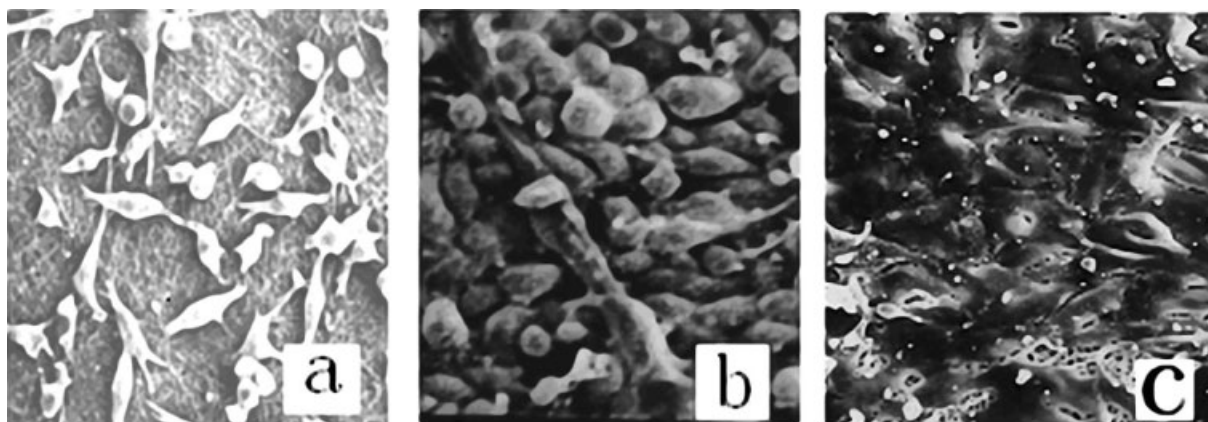
#### SEM

Figure 7(a) showed HUVECs crosslinked with the SF/gelatin nanofiber membranes after 5 days of cultivation. Most cells were shuttle-shape and coterminous. They adhered and spread on the surface of SF/gelatin nanofibers. Figure 7(b) showed HUVECs interacted and integrated well with the surrounding fibers after 21 days, formed a three-dimensional network of the nanofibrous structure and grew in the direction of fiber orientation as shown in Figure 7(c). All these results indicate that the electrospun scaffolds can support long-term cell growth, proliferation, and adhesion.

### CONCLUSIONS

With the addition of gelatin, SF/gelatin blend solution has excellent spinnability. FTIR and DTA analysis of SF, SF/gelatin nanofibers showed that the structures of  $\beta$ -sheet increased with the addition of gelatin, so its mechanical properties improved. The breaking tenacity of the blend nanofiber scaffolds (70 : 30 w/w, the concentration 13%) was up to 1.60 MPa. The strain at break was 7.6%, porosity was 87%, and average pore diameter was 142 nm. Nanofiber morphology was homogeneous and the average diameter reached 89.2 nm.

HUVECs and mouse fibroblasts seeded on the SF/gelatin nanofibrous scaffolds had more spreading and proliferation than that on the pure SF nanofiber scaffolds. These blended scaffolds can replace the natural ECM proteins, support long-term cell growth, form three-dimensional networks of



**Figure 7** SEM images of HUVECs after 5 days (a) and 21 days (b, c) of cultivation on the SF/gelatin membranes.

nanofibrous structure, and grow in the direction of fiber orientation.

All the results proved that the electrospun SF/gelatin nanofiber membranes, which had the ability of mimicking the structure and component of ECM, could promote the growth and proliferation of mouse fibroblasts and HUVECs exist in the native vessels. Therefore, the electrospun SF/gelatin nanofiber membranes have a tremendous potential for blood vessel engineering scaffolds. This article provided basic research for the electrospun SF/gelatin nanofiber membranes used as scaffolds. Further research will form tubular scaffolds by a rotating mandrel-type collector and deeply explore the feasibility for blood vessel engineering materials.

The authors are indebted to the Testing Center of Soochow University for the use of the TGA-DSC and FTIR instruments.

## References

1. Kim, S. H.; Nam, Y. S.; Lee, T. S. *Polymer* 2003, 35, 185.
2. Min, B.-M.; Lee, G. *Biomaterials* 2004, 5, 1289.
3. Kobayashi, T. *Foods Food Ingredients Jpn* 1996, 170, 82.
4. Zhang, Y. Z.; Venugopal, J.; Huang, Z.-M. *Polymer* 2006, 47, 2911.
5. Vaz, C. M.; van Tuijl, S.; Bouten, C. V. C. *Acta Biomater* 2005, 1, 575.
6. Hea, W.; Ma, Z. *Biomaterials* 2005, 26, 7606.
7. Jin, H.-J.; Chen, J.; Karageorgiou, V. *Biomaterials* 2004, 25, 1039.
8. Um I. C.; Kweon, H. Y.; Lee, K. G.; Park, Y. H. *Int Biol Macromol* 2003, 33, 203.
9. Jeong, L.; Lee, K. Y.; Liu, J. W. *Int J Biol Macromol* 2006, 38, 140.
10. Ki, C. S.; Baek, D. H.; Gang, K. D. *Polymer* 2005, 46, 509.
11. Magoshi, J.; Magoshi, Y. *J Polym Sci Polym Phys Ed* 1977, 15, 1675.
12. Iniuta, N. M.; Saiba, M.; Iguchi, H. *Biochem Biophys Res Commun* 1995, 208, 511.